

Lyapunov-Based Control of a Nonlinear Multiagent System With a Time-Varying Input Delay Under False-Data-Injection Attacks

Arman Sargolzaei , Brendon C. Allen , Carl D. Crane, and Warren E. Dixon

Abstract—This article introduces a Lyapunov-based nonlinear control scheme that mitigates false-data-injection (FDI) attacks in real time for a centralized multiagent system (MAS) with nonlinear Euler–Lagrange dynamics with additive disturbances and input delays. Since the state tracking error is faulty during FDI attacks, the central controller cannot solely rely on the state tracking error to coordinate the MAS. Therefore, a novel feedback signal is designed to address this challenge and to ensure that the MAS achieves the control objective. The proposed controller combines both learning and model-based approaches to estimate the agents’ states and to detect and respond to FDI attacks. A neural network (NN) is used to detect the FDI attacks, where the update laws for the NN weights are designed based on the corresponding stability analysis. Lyapunov–Krasovskii functionals are used in the Lyapunov-based stability analysis to ensure semi-global uniformly ultimately bounded tracking. A simulation of multiagent robots with nonlinear Euler–Lagrange dynamics is provided, demonstrating the promising performance of the developed method to respond to FDI attacks.

Index Terms—Euler–Lagrange system, false-data-injection attack, Lyapunov–Krasovskii, nonlinear systems, time-varying input delay.

I. INTRODUCTION

IN a centralized multiagent system (MAS), agents share their data with a central processing unit and receive control commands. Centralized MASs are extensively used in industrial applications such as load frequency control of smart grid systems, formation flight, manufacturing automation, and search and rescue [1], [2]. The physics of such systems can be modeled by general Euler–Lagrange (EL) dynamics. Furthermore, due

Manuscript received February 12, 2021; revised April 18, 2021 and July 10, 2021; accepted August 6, 2021. Date of publication August 19, 2021; date of current version December 27, 2021. This work was supported in part by AFOSR under Grant FA9550-19-1-0169. Paper no. TII-21-0278. (Corresponding author: Arman Sargolzaei.)

Arman Sargolzaei is with the Department of Mechanical Engineering, Tennessee Technological University, Cookeville, TN 38505 USA (e-mail: a.sargolzaei@gmail.com).

Brendon C. Allen, Carl D. Crane, and Warren E. Dixon are with the Department of Mechanical and Aerospace Engineering, University of Florida, Gainesville, FL 32611 USA (e-mail: brendoncallen@ufl.edu; crane@ufl.edu; wdixon@ufl.edu).

Color versions of one or more figures in this article are available at <https://doi.org/10.1109/TII.2021.3106009>.

Digital Object Identifier 10.1109/TII.2021.3106009

to communication constraints, control signals are transmitted to the agents with time-varying delays, which can significantly degrade the performance or destabilize the MAS under certain conditions. This article presents the design and analysis of an observer/controller and investigates the robustness of such practical dynamic systems. The performance of the closed-loop systems is examined through a numerical simulation for a set of coordinated robot manipulators.

The use of a communication network between agents gives a MAS a distinct advantage in terms of efficiency, design cost, and simplicity. However, this benefit comes at the expense of increased vulnerability to a range of cyber-physical attacks such as false-data-injection (FDI) attacks. An adversary can inject an FDI attack by gaining access to the communication channels and injecting faults to the information transmitted from the agents to the control center. The vulnerability of control systems to FDI attacks have been well established in the literature [3], [4]. Further, the adverse impact of FDI attacks on nonlinear systems has been discussed in the literature [5]. Thus, the performance of the MAS is disrupted in the presence of FDI attacks. Therefore, it is essential to design control systems that can detect and provide resilience to FDI attacks.

There has been progressive development of novel detection mechanisms to FDI attacks imposed on a MAS. FDI attack detection can be classified into model-based methods [6]–[11] and learning-based methods [12]–[18]. Model-based methods use an observer to estimate the system’s dynamics. For example, an adaptive sliding-mode observer with online parameter estimation is used to detect state and sensor attacks in [6]. Manandhar *et al.* [10] designed a Kalman filter estimator as well as a means to detect different types of faults and cyber-attacks, such as FDI attacks. Deng *et al.* [8] designed a least-budget defense strategy to protect control systems under an FDI attack. Principal component analysis (PCA) was used in [9] and [19] to ensure data integrity during state estimation of control systems. Despite the advantages of model-based methods, including real-time anomaly detection and low computational complexity, pure dependency on a mathematical model makes them vulnerable to model uncertainties and disturbances. Such uncertainties could be alleviated by learning-based methods (e.g., artificial neural networks (NNs) [12]–[14] and machine learning algorithms [15]–[18]) that can estimate complex nonlinear functions. However, learning-based methods often require extensive training, which presents a challenge for real-time detection of an

FDI attack. In this article, a detection and estimation strategy is developed by combining model and learning-based techniques, which increases the accuracy of estimation and does not require extensive offline training.

Of the prior efforts to mitigate FDI attacks on control systems, few investigated the real-time detection and mitigation of FDI attacks and each only considered systems with linear dynamics [3], [4], [20]–[22]. The work in [20] proposed a secure hybrid dynamic-state estimation approach that is designed based on an unknown input observer. The work in [3] suggested a likelihood ratio test in response to FDI attacks, which are injected for a short period and cannot be identified using threshold-based detection algorithms. State-estimation-based techniques are used in [4] to mitigate FDI attacks. The work in [21] developed a simultaneous input and state estimation-based algorithm to mitigate FDI attacks injected into the measurements of a control system. The proposed technique considered the FDI attack signal as an unknown input and designed a state estimator to compensate for the FDI attack. The work in [22] proposed a mitigation algorithm using a Kalman filter for networked control systems under FDI attacks. The algorithm used an NN-based architecture to detect and mitigate FDI attacks in real-time. However, the aforementioned results rely on an accurate system model and only considered linear systems.

FDI compensation for nonlinear systems is inherently more challenging. Therefore, few methods have been developed for such systems [5], [23]–[26]. An FDI attack mitigation approach is developed in [5] for a class of nonlinear systems based on a retrospective cost-based adaptive controller; however, the method only works when the FDI attack is injected into the actuator signals. A nonlinear-based observer is developed in [23] to detect and mitigate faults injected into sensors and actuators of a control system. The proposed approach in [23] used an NN-based technique to detect injected faults in real time. However, the stability of the designed controller has not been investigated. The work in [24] developed an adaptive control approach for a class of nonlinear systems under FDI attacks. A stable controller is developed in [25] and [27] for a class of nonlinear systems but is limited to random and impulsive deception attacks. The work in [26] proposed a resilient state estimation scheme for nonlinear systems under sensor attack. The developed scheme can detect sensor attacks in real time, but compensation requires further investigation.

Lyapunov–Krasovskii (LK) functionals are often used to investigate the stability of nonlinear systems with actuator delays. LK functionals are used in [28] to ensure the stability of controllers for an EL system subjected to delayed actuation and additive bounded disturbances. The work was extended in [29] to include a time-varying input delay. A Lyapunov-based controller was developed in [30] for a nonlinear system with an uncertain time-varying input delay and additive disturbances. However, since FDI attacks are added into the measurement signals by an adversary, the main technical challenge is that the state tracking error is not measurable under FDI attacks. Therefore, the results in [28]–[30] are not practical during FDI attacks, since their controllers include the state tracking error.

To address this challenge, we develop alternative auxiliary error signals that are always measurable, despite the injection of FDI attacks, and can be used to facilitate the objective.

To the best of our knowledge, previous methods cannot generate robustness to FDI attacks for MASs composed of agents with EL nonlinear dynamics under disturbances and input delays. Therefore, the contributions of this article include the following: 1) a real-time FDI attack detection and compensation scheme is developed for a centralized MAS featuring agents with nonlinear EL dynamics, 2) a secure Lyapunov-based control strategy is designed for a class of nonlinear systems with input delays that is robust to the injection of FDI attacks, additive disturbances, and measurement noise, and 3) the stability of the proposed controller is investigated to prove that the tracking errors converge to a steady-state residual.

There has been a notable increase in the use of centralized MASs in robotic applications. Applications vary from performing usual tasks in manufacturing to space exploration [31]–[34]. In addition, the physics of these systems and a large class of industrial systems such as electromechanical systems and cyber-physical systems can be modeled with EL dynamics. Due to the increased application of two-link planar manipulators in industrial applications, and the recent focus of the Lyapunov-based control of such systems [35]–[40], the developed algorithm is implemented and assessed on a centralized MAS composed of two-link, revolute, and planar manipulators. This model illustrates the developed design’s capability of controlling a nonlinear system with EL dynamics under additive disturbances, measurement noise, FDI attacks, and also input delayed.

The rest of the article is organized as follows. A centralized MAS under an FDI attack is formulated in Section II. The objectives of the article are described in Section III. The error signals and the Lyapunov-based controller are developed in Section IV. The proposed FDI attack estimation algorithm is introduced in Section V. Section VI provides the stability analysis of the designed controller and estimator. The performance of the proposed secure nonlinear controller is evaluated for a case study, and the results are shown in Section VII. Finally, Section VIII concludes this article.

II. DYNAMIC MODEL

Fig. 1 illustrates the structure of a centralized MAS under FDI attacks. The centralized MAS has $N \in \mathbb{Z}_{>0}$ agents indexed by $\mathcal{V} \triangleq \{1, 2, \dots, N\}$. The communication topology of the centralized MAS is modeled as a static and undirected star graph $\mathcal{G} \triangleq (\mathcal{V}, \mathcal{E})$, where $\mathcal{E} \subseteq \mathcal{V} \times \mathcal{V}$ denotes the edge set and \mathcal{V} denotes the node set. The central node represents the control center in the figure, and the outer nodes represent the agents. The graph, \mathcal{G} , is assumed to be connected $\forall t \geq t_0$. In the centralized MAS, agent i transmits measurable states, x_i , to the control center, where a corresponding control input is computed and is transmitted back to agent i .

Remark 1: Throughout the article, time-varying delayed functions $\zeta_i(t - \tau_i(t))$ are represented by ζ_{τ_i} , where τ_i denotes the time-varying time-delay.

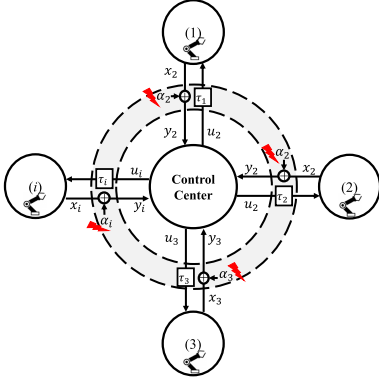


Fig. 1. Illustration of a centralized MAS subject to FDI attacks. A star graph communication topology is considered in this work. The central node denotes the centralized controller, and the external nodes indicate the agents. The communication links are shown with dashed lines. The control and state feedback signals are shown by solid lines subjected to known time-delays and FDI attacks, respectively. In this figure, the lightning bolt represents the FDI attack.

A. MAS With Input Delay Under FDI Attacks

Each agent is modeled as an EL dynamic system. The dynamic model of agent $i \in \mathcal{V}$ is [41]

$$\begin{aligned} M_i(q_i)\ddot{q}_i + V_i(q_i, \dot{q}_i)\dot{q}_i + G_i(q_i) + F_i(\dot{q}_i) + d_i(t) &= u_{\tau_i} \\ y_i(t) &= \pi_i(q_i, S_{1_i}) \\ \dot{y}_i(t) &= \pi_i(\dot{q}_i, S_{2_i}) \end{aligned} \quad (1)$$

where n_i represents the number of states for agent i , $q_i, \dot{q}_i, \ddot{q}_i : [t_0, \infty) \rightarrow \mathbb{R}^{n_i}$ represent the generalized states, $t_0 \in \mathbb{R}_{\geq 0}$ represents the initial time, $M_i \in \mathbb{R}^{n_i \times n_i}$ represents the known generalized inertia matrix, $V_i \in \mathbb{R}^{n_i \times n_i}$ represents the known generalized centripetal-Coriolis matrix, $G_i \in \mathbb{R}^{n_i}$ represents the known generalized gravity vector, $F_i \in \mathbb{R}^{n_i}$ represents the known generalized friction function, $d_i : [t_0, \infty) \rightarrow \mathbb{R}^{n_i}$ represents a bounded exogenous disturbance, $u_{\tau_i} : [t_0, \infty) \rightarrow \mathbb{R}^{n_i}$ represents the generalized delayed control input, $\tau_i : [t_0, \infty) \rightarrow \mathbb{R}_{>0}$ represents a known time-varying delay, $y_i, \dot{y}_i : [t_0, \infty) \rightarrow \mathbb{R}^{n_i}$ represent the state measurements under FDI attacks, $\pi_i \in \mathbb{R}^{n_i}$ is a known output function, and $S_{1_i}, S_{2_i} \in \mathbb{R}^{n_i}$ account for the FDI attacks and the measurement noise.

Assumption 1: The reference trajectory, $q_{d_i} : [t_0, \infty) \rightarrow \mathbb{R}^{n_i}$ is designed such that it and its first and second derivatives are bounded by known positive constants, i.e., $q_{d_i}, \dot{q}_{d_i}, \ddot{q}_{d_i} \in \mathcal{L}_{\infty}$ [42].

Assumption 2: The disturbance is continuous and bounded by a known constant, i.e., $\|d_i(t)\| < \bar{d}_i \forall t \geq t_0$, where $\bar{d}_i \in \mathbb{R}_{>0}$ [42].

Assumption 3: The matrix, M_i , is symmetric, positive-definite, and satisfies the following inequality:

$$\underline{m}_i \|\Gamma_i\|^2 \leq \Gamma_i^T M_i \Gamma_i \leq \bar{m}_i \|\Gamma_i\|^2, \forall \Gamma_i \in \mathbb{R}^{n_i} \quad (2)$$

where \underline{m}_i and \bar{m}_i are known positive constants [42]. Moreover, the inverse or pseudo-inverse of M is C^1 and bounded.¹

¹ C^k represents the set of k -continuously differentiable functions for $k \in \mathbb{Z}_{>0}$.

Assumption 4: The time-varying input delay is bounded and differentiable such that $\tau_i(t) < \bar{\tau}_i, \forall t \in \mathbb{R}_{>0}$, where $\bar{\tau}_i$ is a positive constant. The rate of change for the delay is bounded such that $|\dot{\tau}_i(t)| < \dot{\tau}_{Max} < 1, \forall t \in \mathbb{R}_{>0}$, where $\dot{\tau}_{Max}$ is a positive constant [43].²

B. False-Data-Injection Attack

Although detection and compensation of FDI attacks have been investigated, prior results have exploited the properties of linear systems, and detection and compensation for the more generalized nonlinear dynamic problem remain an open challenge. Because many practical MAS systems also experience input delays, the development in this article considers general input-delayed EL dynamics. Often the goal of an adversary is to inject incorrect information to disrupt the stable operation of the system while the system's detection mechanism remains unaware of the attack. In general, injected false data that is not within the system's operating limit is detectable by using anomaly detection algorithms. Thus, an intelligent adversary injects false data close to the nominal states of the system. As a result, such FDI attacks are bounded and are much more challenging to detect.

In this article, an FDI attack and measurement noise are modeled by a function $\pi_i : [t_0, \infty) \rightarrow \mathbb{R}^{n_i}$, which alters the measured feedback signals as

$$\begin{cases} \pi_i(q_i, S_{1_i}) \triangleq q_i(t) + S_{1_i}(t) \\ \pi_i(\dot{q}_i, S_{2_i}) \triangleq \dot{q}_i(t) + S_{2_i}(t) \end{cases} \quad (3)$$

where $S_{j_i} \triangleq \alpha_{j_i}(t) + \theta_{j_i}(t) \in \mathbb{R}^{n_i}$ for $j = \{1, 2\}$, $\alpha_{1_i}(t) \in \mathbb{R}^{n_i}$ and $\alpha_{2_i}(t) \in \mathbb{R}^{n_i}$ are unknown, bounded, time-varying, and continuous faults, which represent FDI attacks on the states of agent i , and $\theta_{1_i}(t)$ and $\theta_{2_i}(t)$ represent Gaussian measurement noise.

Assumption 5: For all $i \in \mathcal{V}$, $S_{1_i}(t)$ and $S_{2_i}(t)$ are differentiable and bounded, i.e., $|S_{j_i}(t)| \leq \bar{S}_{j_i} \forall t \geq t_0, j = \{1, 2\}$, where \bar{S}_{1_i} and \bar{S}_{2_i} are known positive constants.

III. PROBLEM STATEMENT

The primary objective is to design a continuous centralized controller to regulate the nonlinear dynamic MAS in (1) to a desired trajectory despite additive bounded disturbances, measurement noise, a time-varying input-delay, and FDI attacks. The error between the state, q_i , and the desired trajectory, $q_{d_i} : [t_0, \infty) \rightarrow \mathbb{R}^{n_i}$, is defined as

$$e_i \triangleq q_{d_i} - q_i \quad (4)$$

where $e_i : [t_0, \infty) \rightarrow \mathbb{R}^{n_i}$ is unmeasurable during an FDI attack. The unique challenge is to ensure accurate tracking for all time, even during an FDI attack. The centralized control algorithm can only measure each agent's outputs, y_i and \dot{y}_i , which are corrupted during an FDI attack. To address this challenge, our second objective is to design a nonlinear observer to estimate

²In practice, the bound for the time-varying input delay can be estimated from experiments.

the MAS's states in real time. The state estimate error, $\tilde{q}_i : [t_0, \infty) \rightarrow \mathbb{R}^{n_i}$, is defined as

$$\tilde{q}_i \triangleq q_i - \hat{q}_i \quad (5)$$

where $\hat{q}_i : [t_0, \infty) \rightarrow \mathbb{R}^{n_i}$ is the state estimate of the i th agent. Another challenge is that when the control signals are transmitted to the agents, a known time-varying delay occurs. To obtain a delay-free control signal in the closed-loop system, an auxiliary signal, $e_{u_i} : [t_0, \infty) \rightarrow \mathbb{R}^{n_i}$, is defined as

$$e_{u_i} \triangleq \int_{t-\tau_i}^t u_i(s) ds. \quad (6)$$

To facilitate the subsequent stability analysis, the following auxiliary errors are defined as

$$r_i \triangleq \dot{c}_i + \beta_i e_i - A_i e_{u_i} \quad (7)$$

and

$$\tilde{r}_i \triangleq \dot{\tilde{q}}_i + \beta_i \tilde{q}_i. \quad (8)$$

In (7) and (8), $r_i : [t_0, \infty) \rightarrow \mathbb{R}^{n_i}$ is a tracking error that is unmeasurable during an FDI attack, $\beta_i \in \mathbb{R}_{>0}$ is a known constant gain, $\tilde{r} : [t_0, \infty) \rightarrow \mathbb{R}^{n_i}$ is an auxiliary estimation error, and $A_i(q_{d_i}) \triangleq M_i^{-1}(q_{d_i}) \in \mathbb{R}^{n_i \times n_i}$ is a known matrix, which satisfies the following inequalities:

$$\|A_i\|_\infty \leq a_i, \|\dot{A}_i\|_\infty \leq a_{d_i} \quad (9)$$

where $a_i, a_{d_i} \in \mathbb{R}_{>0}$ are known constants. The error between $M_i^{-1}(q_i)$ and $A_i(q_{d_i})$ is represented by $\eta_i : [t_0, \infty) \rightarrow \mathbb{R}^{n_i \times n_i}$ and is defined as

$$\eta_i \triangleq A_i(q_{d_i}) - M_i^{-1}(q_i). \quad (10)$$

The expression in (10) satisfies the following inequality:

$$\|\eta_i\|_\infty \leq \bar{\eta}_i \quad (11)$$

where $\bar{\eta}_i \in \mathbb{R}_{>0}$ is a known constant.

Since the tracking error in (7) cannot be used for the closed-loop control design, our challenge is to develop a measurable feedback signal, which remains unaffected by the injection of FDI attacks. To address this, we developed a tracking error $\hat{r}_i : [t_0, \infty) \rightarrow \mathbb{R}^{n_i}$, which is defined as

$$\hat{r}_i \triangleq \dot{\Psi}_{1_i} + \beta_i \Psi_{1_i} - A_i e_{u_i} + \hat{S}_i \quad (12)$$

where $\Psi_{1_i} \triangleq q_{d_i} - y_i$ is a measurable feedback signal, and $\hat{S}_i \in \mathbb{R}^{n_i}$ is a subsequently designed FDI attack estimate.

Problem Statement Given the dynamic model of agent i in (1), a centralized MAS modeled by \mathcal{G} , Assumptions 1–5, and the injection of FDI attacks modeled in (3), design a continuous controller, observer, and FDI attack estimator to ensure that e_i in (4) is uniformly ultimately bounded (UUB) for each agent $i \in \mathcal{V}$.

IV. CONTROLLER AND OBSERVER DEVELOPMENT

The open-loop tracking error of agent i is obtained by taking the time derivative of (7), multiplying by M_i , and substituting

(1) to yield

$$M_i \dot{r}_i \triangleq M_i \ddot{q}_{d_i} + V_i \dot{q}_i + G_i + F_i + d_i + \beta_i M_i \dot{e}_i - u_{\tau_i} - \dot{A}_i e_{u_i} - M_i A_i [u_i - (1 - \dot{\tau}_i) u_{\tau_i}]. \quad (13)$$

Based on the subsequent stability analysis, the controller is designed as

$$u_i \triangleq k_i \hat{r}_i \quad (14)$$

where $k_i \in \mathbb{R}_{>0}$ is a known user-defined control gain. Using (1), (3), (4), (7), and (12), \hat{r}_i can be written as

$$\hat{r}_i = r_i - N_i \quad (15)$$

where $N_i : [t_0, \infty) \rightarrow \mathbb{R}^{n_i}$ represents the FDI attack estimation error and is defined as

$$N_i \triangleq S_i - \hat{S}_i \quad (16)$$

where $S_i \triangleq S_{2_i} + \beta_i S_{1_i}$ is an auxiliary term related to the FDI attacks.

Substituting (14) into (13), and using (15) yields

$$M_i \dot{r}_i = -\frac{1}{2} \dot{M}_i r_i + \chi_{1_i} + N_{1_i} - k_i r_i - k_i \dot{\tau}_i r_{\tau_i} - k_i M_i \eta_i r_i + k_i M_i \eta_i k_{1_i} r_{\tau_i} - e_i + \beta_i M_i A_i e_{u_i} - \dot{A}_i e_{u_i} \quad (17)$$

where $k_{1_i} \triangleq 1 - \dot{\tau}_i$ and $\chi_{1_i}, N_{1_i} \in \mathbb{R}^{n_i}$ are auxiliary terms which are defined as

$$\chi_{1_i} \triangleq M_i \ddot{q}_{d_i} + V_i \dot{q}_i + G_i + F_i - N_{1_d_i} + \beta_i M_i r_i - \beta_i^2 M_i e_i + \frac{1}{2} \dot{M}_i r_i + e_i \quad (18)$$

and

$$N_{1_i} \triangleq N_{1_d_i} + k_i N_i + k_i \dot{\tau}_i N_{\tau_i} + k_i M_i \eta_i N_i - k_i M_i \eta_i k_{1_i} N_{\tau_i} + d_i \quad (19)$$

respectively, and $N_{1_d_i} \in \mathbb{R}^{n_i}$ is defined as

$$N_{1_d_i} \triangleq M_{d_i} \ddot{q}_{d_i} + V_{d_i} \dot{q}_{d_i} + G_{d_i} + F_{d_i} \quad (20)$$

where $M_{d_i}, V_{d_i}, G_{d_i}$, and F_{d_i} represent $M_i(q_{d_i}) \in \mathbb{R}^{n_i \times n_i}$, $V_i(q_{d_i}, \dot{q}_{d_i}) \in \mathbb{R}^{n_i \times n_i}$, $G_i(q_{d_i}) \in \mathbb{R}^{n_i}$, and $F_i(\dot{q}_{d_i}) \in \mathbb{R}^{n_i}$, respectively.

To facilitate the state estimation design, (1) can be written in the advantageous form

$$\ddot{q}_i = f_i(q_i, \dot{q}_i) + g_i(q_i) u_{\tau_i} - d_{1_i} \quad (21)$$

where $f_i(q_i, \dot{q}_i) \triangleq -g_i(q_i)[V_i(q_i, \dot{q}_i)\dot{q}_i + G_i(q_i) + F_i(\dot{q}_i)]$, $g_i \triangleq M_i^{-1}$, and $d_{1_i} \triangleq M_i^{-1} d_i$ represent a bounded exogenous disturbance. Based on the form of (21), the state estimate of agent i is designed as

$$\ddot{\hat{q}}_i \triangleq f_i(\hat{q}_i, \dot{\hat{q}}_i) + A_i u_{\tau_i} - L_{1_i} \Psi_{2_i} + L_{2_i} \Psi_{3_i} \quad (22)$$

where $L_{1_i}, L_{2_i} \in \mathbb{R}_{>0}$ denote constant user-defined observer gains, and $\Psi_{2_i}, \Psi_{3_i} : [t_0, \infty) \rightarrow \mathbb{R}^{n_i}$ denote measurable observer feedback signals which are designed based on the subsequent stability analysis as

$$\Psi_{2_i} \triangleq \dot{y}_i + \beta_i y_i - \dot{\hat{q}}_i - \beta_i \hat{q}_i - \hat{S}_i \quad (23)$$

and

$$\Psi_{3_i} \triangleq \dot{q}_{d_i} - \dot{\hat{q}}_i + \beta_i(q_{d_i} - \hat{q}_i) - A_i e_{u_i}. \quad (24)$$

The closed-loop estimation error can be obtained by substituting (21) and (22) into the time derivative of (8) as

$$\dot{\tilde{r}}_i = -L_{2_i} \tilde{r}_i - k_i \eta_i r_{\tau_i} - \tilde{q}_i + \chi_{2_i} + N_{2_i} + L_{1_i} (S_i - \hat{S}_i) \quad (25)$$

where $\chi_{2_i}, N_{2_i} \in \mathbb{R}^{n_i}$ are defined as

$$\begin{aligned} \chi_{2_i} \triangleq & f_i(q_i, \dot{q}_i) - f_i(\hat{q}_i, \dot{\hat{q}}_i) + \beta_i \tilde{r}_i + L_{1_i} \tilde{r}_i - L_{2_i} r_i \\ & - \beta_i^2 \tilde{q}_i + \tilde{q}_i \end{aligned} \quad (26)$$

and

$$N_{2_i} \triangleq k_i \eta_i N_{\tau_i} - d_{1_i}. \quad (27)$$

By using the mean value theorem (MVT) and Assumptions 1 and 2, an upper bound can be found for the expressions in (18) and (26) as $\|\chi_{1_i}\| \leq \rho_{1_i}(\|z_i\|)\|z_i\|$ and $\|\chi_{2_i}\| \leq \rho_{2_i}(\|z_i\|)\|z_i\|$, where $\rho_{1_i}(\|z_i\|)$ and $\rho_{2_i}(\|z_i\|)$ are positive, globally invertible, nondecreasing functions [41], and $z_i \in \mathbb{R}^{4n_i}$ is defined as

$$z_i \triangleq [e_i^T, r_i^T, \tilde{q}_i^T, \tilde{r}_i^T]^T. \quad (28)$$

V. FDI ATTACK ESTIMATION

This section presents the proposed anomaly detection algorithm. Notice that the developed observer in (22) includes a nonlinear state estimator and an NN-based FDI attack detection algorithm, which enables state estimation of the agents in real time. Since the unknown FDI attack function, S_i , is over a noncompact domain, the following nonlinear mapping, $f_{s_i} : [t_0, \infty) \rightarrow [0, 1]$, is defined to map time to a compact spatial domain [44]:

$$f_{s_i} \triangleq \frac{k_{s_i}(t - t_0)}{k_{s_i}(t - t_0) + 1}, \xi \in [0, 1], t \in [t_0, \infty) \quad (29)$$

where $k_{s_i} \in \mathbb{R}_{>0}$ is a user-defined saturation gain. Observe that $f_{s_i}^{-1} : [0, 1] \rightarrow [t_0, \infty)$, defined as

$$f_{s_i}^{-1}(\xi) = \frac{k_{s_i} t_0 (1 - \xi) + \xi}{k_{s_i} (1 - \xi)}$$

is the inverse of f_{s_i} . Thus, the FDI attack function, $S_i(t)$, can be mapped into the compact domain, ξ , as

$$S_i(t) = S_i(f_{s_i}^{-1}(\xi)) \triangleq S_{f_{s_i}}(\xi). \quad (30)$$

Since $S_{f_{s_i}} : [0, 1] \rightarrow \mathbb{R}^{n_i}$ is a continuous function that is defined over a compact domain, the Stone–Weierstrass theorem in [45] is satisfied, and (30) can be expressed as

$$S_{f_{s_i}}(\xi) = W_i^T \sigma(V_i^T \delta_i) + \varepsilon_i \quad (31)$$

where $\varepsilon_i \in \mathbb{R}^{n_i}$ is bounded such that $\|\varepsilon_i\| \leq \bar{\varepsilon}_i \in \mathbb{R}_{>0}$, where $\bar{\varepsilon}_i$ is a known constant, the vectors $W_i \in \mathbb{R}^{(n_n+1) \times n_i}$ and $V_i \in \mathbb{R}^{(n_i+1) \times n_n}$ consist of the ideal unknown constant learning weights, n_n is the number of neurons in the hidden layer, $\delta_i \in \mathbb{R}^{(n_i+1) \times 1}$ represents the inputs into the NN, and $\sigma(\cdot) \in$

$\mathbb{R}^{(n_n+1)}$ represents a stacked vector of activation functions, which are selected to be C^2 [46].

Based on (31), the NN approximation for the FDI attack on agent i with respect to the spatial domain $[0, 1]$ is represented by $(\hat{S}_i \circ f_{s_i}^{-1}) : [0, 1] \rightarrow \mathbb{R}^{n_i}$ and defined by

$$\hat{S}_i \triangleq \hat{W}_i^T \sigma(\hat{V}_i^T \delta_i) \quad (32)$$

where the vectors $\hat{W}_i \in \mathbb{R}^{(n_n+1) \times n_i}$, $\hat{V}_i \in \mathbb{R}^{(n_i+1) \times n_n}$ are estimates of the ideal learning weights, and δ_i is defined as

$$\delta_i \triangleq [1, \Psi_{2_i}^T]^T. \quad (33)$$

Substituting (30)–(32) into (16) yields

$$N_i = W_i^T(t) \sigma(V_i^T(t) \delta_i(t)) - \hat{W}_i^T(t) \sigma(\hat{V}_i^T(t) \delta_i(t)) + \varepsilon_i. \quad (34)$$

Using a Taylor's series approximation, the expression in (34) can be written as

$$N_i = \tilde{W}_i^T \sigma(\hat{V}_i^T \delta_i) + \hat{W}_i^T \sigma'(\hat{V}_i^T \delta_i) \tilde{V}_i^T \delta_i + N_{n_i} \quad (35)$$

where

$$N_{n_i} \triangleq \tilde{W}_i^T \sigma'(\hat{V}_i^T \delta_i) \tilde{V}_i^T \delta_i + W_i^T \mathcal{O}(\tilde{V}_i^T \delta_i) + \varepsilon_i \quad (36)$$

where $\tilde{W}_i = W_i - \hat{W}_i$ denotes the outer NN weight error, $\tilde{V}_i = V_i - \hat{V}_i$ denotes the inner NN weight error, \mathcal{O} denotes higher order terms, and $\|N_{n_i}\| \leq \bar{n}_{n_i}$ for some $\bar{n}_{n_i} \in \mathbb{R}_{>0}$.

Based on the subsequent stability analysis, \hat{W}_i and \hat{V}_i are designed as

$$\dot{\hat{W}}_i = \text{proj} \left(\Gamma_{1_i} L_{1_i} \sigma(\hat{V}_i^T \delta_i) \Psi_{2_i}^T \right) \quad (37)$$

and

$$\dot{\hat{V}}_i = \text{proj} \left(\Gamma_{2_i} L_{1_i} \delta_i \Psi_{2_i}^T \hat{W}_i^T \sigma'(\hat{V}_i^T \delta_i) \right) \quad (38)$$

where $\Gamma_{1_i}, \Gamma_{2_i} \in \mathbb{R}^{n_i \times n_i}$ are constant diagonal positive definite matrices, and the function $\text{proj}(\cdot)$ represents the Lipschitz continuous projection operator defined in [47], which is used to ensure that \hat{W}_i and \hat{V}_i remain bounded. Recall that $S(t)$ is bounded based on Assumption 5. Moreover, since \hat{W}_i and $\sigma(\hat{V}_i^T \delta_i)$ are bounded by construction, then from (32), \hat{S}_i is bounded, and therefore, from (16), the FDI attack estimation error, N_i , is bounded as

$$\|N_i\| \leq \bar{n}_i, \forall t \geq t_0, i \in \mathcal{V} \quad (39)$$

where $\bar{n}_i \in \mathbb{R}_{>0}$ is a known constant. Furthermore, Assumptions 1 and 2 are used to obtain the following inequalities for (19) and (27):

$$\|N_{1_i}\| \leq \bar{n}_{1_i}, \|N_{2_i}\| \leq \bar{n}_{2_i} \quad (40)$$

where $\bar{n}_{1_i}, \bar{n}_{2_i} \in \mathbb{R}_{>0}$ are known constants.

A block diagram for the proposed control strategy is shown in Fig. 2.

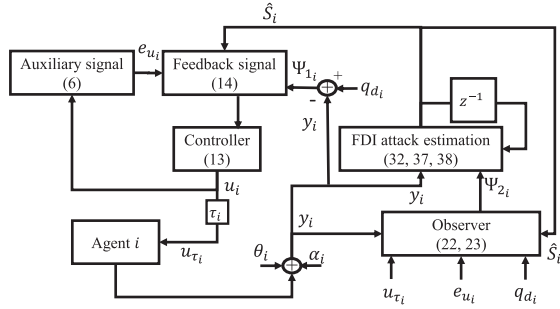


Fig. 2. Overview of the proposed control strategy.

VI. STABILITY ANALYSIS

Let $\Pi_i \in \mathbb{R}^{4n_i+3}$ be defined as

$$\Pi_i \triangleq [z_i^T, \sqrt{P_{LK_i}}, \sqrt{Q_{LK_i}}, \sqrt{R_{LK_i}}]^T \quad (41)$$

where $P_{LK_i}, Q_{LK_i}, R_{LK_i} : [t_0, \infty) \rightarrow \mathbb{R}_{\geq 0}$ are LK functionals defined as

$$P_{LK_i} \triangleq \omega_{1_i} \int_{t-\tau_i}^t \left(\int_{\theta}^t \|u_i(s)\|^2 ds \right) d\theta \quad (42)$$

$$Q_{LK_i} \triangleq \omega_{2_i} \int_{t-\tau_i}^t \|r_i(s)\|^2 ds \quad (43)$$

$$R_{LK_i} \triangleq \omega_{3_i} \int_{t-\tau_i}^t \left(\int_{\theta}^t \|r_i(s)\|^2 ds \right) d\theta \quad (44)$$

and $\omega_{1_i}, \omega_{2_i}, \omega_{3_i} \in \mathbb{R}_{>0}$ are user-defined constants. Let $H_{L_i} : [t_0, \infty) \rightarrow \mathbb{R}_{\geq 0}$ be defined as

$$H_{L_i} \triangleq \frac{1}{2} \text{tr}(\tilde{W}_i^T \Gamma_i^{-1} \tilde{W}_i) + \frac{1}{2} \text{tr}(\tilde{V}_i^T \Gamma_{2_i}^{-1} \tilde{V}_i) \quad (45)$$

where $|H_{L_i}| \leq H_{L_{i,\max}}$ for some $H_{L_{i,\max}} \in \mathbb{R}_{>0}$, since \tilde{W}_i and \tilde{V}_i are bounded. The following sufficient conditions and parameter definitions are presented for the subsequent stability analysis. Let $\epsilon_{p_i} \in \mathbb{R}_{>0}$, for $p \in \{1, 2, \dots, 10\}$, be user-defined parameters that are selected such that the following sufficient conditions are satisfied³:

$$\beta_i > \frac{a_i \epsilon_{1_i}}{2}$$

$$k_i > \left(k_i \bar{m}_i \bar{\eta}_i + \frac{k_i \epsilon_{2_i}}{2} (\dot{\tau}_{Max} + \bar{m}_i \bar{\eta}_i k_{1_i}) + \frac{\epsilon_{9_i}}{2} (a_{d_i} + \beta_i \bar{m}_i a_i) + \frac{\epsilon_{3_i}}{2} + \frac{\epsilon_{4_i}}{2} + \bar{\tau}_i \omega_{1_i} k_i^2 + k_i^2 \bar{\tau}_i \omega_{1_i} \epsilon_{10_i} + \omega_{2_i} + \bar{\tau}_i \omega_{3_i} \right)$$

$$L_{2_i} > \frac{k_i \bar{\eta}_i \epsilon_{5_i}}{2} + \frac{\epsilon_{3_i}}{2} + \frac{\epsilon_{6_i}}{2} + \frac{L_{1_i} \epsilon_{7_i}}{2}$$

$$\omega_{1_i} > \frac{a_i \bar{\tau}_i}{\epsilon_{1_i} k_{1_i}} + \frac{(a_{d_i} + \beta_i \bar{m}_i a_i) \bar{\tau}_i}{\epsilon_{9_i} k_{1_i}}$$

³There exist a set of gains to satisfy all of the gain conditions. For example, the gain conditions can be satisfied using the following gains: $a_i = 4$, $a_{d_i} = 7.55$, $\epsilon_{1_i} = 0.9$, $\beta_i = 2$, $\bar{m}_i = 4$, $\bar{\eta}_i = 0.001$, $k_i = 21$, $\epsilon_{2_i} = 0.99$, $\tau_i = 0.005$, $\dot{\tau}_{Max} = 0.8$, $k_{1_i} = 0.999$, $\epsilon_{9_i} = 0.1$, $\epsilon_{3_i} = \epsilon_{4_i} = 0.0001$, $\omega_{1_i} = 3.18$, $\omega_{2_i} = 9.7$, $\omega_{3_i} = 0.0001$, $\epsilon_{10_i} = 0.00001$, $L_{1_i} = 0.01$, $L_{2_i} = 0.012$, $\epsilon_{5_i} = 0.4$, $\epsilon_{6_i} = \epsilon_{7_i} = 0.00001$.

$$\omega_{2_i} > \frac{k_i \bar{\eta}_i}{2 \epsilon_{5_i} k_{1_i}} + \frac{k_i}{2 \epsilon_{2_i} k_{1_i}} (\bar{m}_i \bar{\eta}_i k_{1_i} + \dot{\tau}_{Max}) \quad (46)$$

where $\epsilon_{j_i} \in \mathbb{R}_{>0} \forall j = 1, \dots, 7$ are known positive adjustable constants.

Let γ_{1_i} and γ_{2_i} be defined as $\gamma_{1_i} \triangleq \min(\frac{1}{2} \bar{m}_i, \frac{1}{2})$, and $\gamma_{2_i} \triangleq \max(\frac{1}{2} \bar{m}_i, 1)$, and let $\beta_{1_i} \triangleq \min\{\alpha_{1_i}, \alpha_{2_i}, \alpha_{3_i}, \beta_i\}$ and $\beta_{2_i} \triangleq \min\{\frac{\beta_{1_i}}{2}, \frac{k_{1_i}}{2 \bar{\tau}_i}, \frac{k_{1_i} \omega_{3_i}}{2 \omega_{2_i}}\}$. Furthermore, based on the sufficient conditions presented in (46), we define the positive constants, α_{p_i} for $p \in \{1, \dots, 5\}$ as

$$\alpha_{1_i} \triangleq \beta_i - \frac{a_i \epsilon_{1_i}}{2} \quad (47)$$

$$\alpha_{2_i} \triangleq k_i - k_i \bar{m}_i \bar{\eta}_i - \frac{k_i \epsilon_{2_i}}{2} (\dot{\tau}_{Max} + \bar{m}_i \bar{\eta}_i k_{1_i}) - \frac{\epsilon_{3_i}}{2} - \frac{\epsilon_{4_i}}{2} - \frac{\epsilon_{9_i}}{2} (a_{d_i} + \beta_i \bar{m}_i a_i) - \tau_i \omega_{3_i} - \omega_{2_i} - \tau_i \omega_{1_i} k_i^2 - k_i^2 \tau_i \omega_{1_i} \epsilon_{10_i} \quad (48)$$

$$\alpha_{3_i} \triangleq L_{2_i} - \frac{k_i \bar{\eta}_i \epsilon_{5_i}}{2} - \frac{\epsilon_{3_i}}{2} - \frac{\epsilon_{6_i}}{2} - \frac{L_{1_i} \epsilon_{7_i}}{2} \quad (49)$$

$$\alpha_{4_i} \triangleq \frac{k_{1_i} \omega_{1_i}}{2 \tau_i} - \frac{a_i}{2 \epsilon_{1_i}} - \frac{(a_{d_i} + \beta_i \bar{m}_i a_i)}{2 \epsilon_{9_i}} \quad (50)$$

$$\alpha_{5_i} \triangleq k_{1_i} \omega_{2_i} - \frac{k_i (\dot{\tau}_{Max} + \bar{m}_i \bar{\eta}_i k_{1_i})}{2 \epsilon_{2_i}} - \frac{k_i \bar{\eta}_i}{2 \epsilon_{5_i}} \quad (51)$$

and let φ_i be defined as

$$\varphi_i \triangleq \frac{\bar{n}_{1_i}^2}{2 \epsilon_{4_i}} + \frac{\bar{n}_{2_i}^2}{2 \epsilon_{6_i}} + \frac{L_{1_i} \bar{n}_{n_i}^2}{2 \epsilon_{7_i}} + \frac{L_{1_i} \epsilon_{8_i} \bar{n}_i^2}{2} + \frac{L_{1_i} \bar{n}_{n_i}^2}{2 \epsilon_{8_i}} + L_{1_i} \bar{n}_i^2 + \frac{2 k_i^2 \bar{\tau}_i \omega_{1_i} \bar{n}_i^2}{2 \epsilon_{10_i}} + \bar{\tau}_i \omega_{1_i} k_i^2 \bar{n}_i^2. \quad (52)$$

The subsequent Lyapunov analysis is performed over the following domain:

$$\mathcal{D}_i \triangleq \left\{ \Pi_i \in \mathbb{R}^{4n_i+3} : \|\Pi_i\| < \inf \left\{ \rho_i^{-1} \left(\left[\sqrt{2 \beta_{2_i} \epsilon_{3_i}}, \infty \right] \right) \right\} \right\}$$

where $\rho_i^2(\|z_i\|) \triangleq \rho_{1_i}^2(\|z_i\|) + \rho_{2_i}^2(\|z_i\|)$ is a positive, globally invertible, nondecreasing function. The set of initial conditions, $\mathcal{S}_{\mathcal{D}_i} \subset \mathcal{D}_i$, is defined as

$$\mathcal{S}_{\mathcal{D}_i} \triangleq \left\{ \Pi_i \in \mathcal{D}_i : \|\Pi_i\| < \sqrt{\frac{\gamma_{1_i} \kappa}{\gamma_{2_i}} - \frac{1}{\gamma_{2_i}} H_{L_{i,\max}}} \right\} \quad (53)$$

where $\kappa \triangleq \inf \left\{ \rho_i^{-1} \left(\left[\sqrt{2 \beta_{2_i} \epsilon_{3_i}}, \infty \right] \right) \right\}^2$. The set $\mathcal{S}_{\mathcal{D}_i}$ can be made arbitrarily large by selecting the gains based on the initial conditions. Hence, the subsequent stability analysis yields a semi-global result. The parameters in (46), γ_{1_i} , and γ_{2_i} should be selected such that the following inequality holds:

$$\sqrt{\frac{1}{\gamma_{1_i}} \left(H_{L_{i,\max}} + \frac{\gamma_{2_i} \varphi_i}{\beta_{2_i}} \right)} < \inf \left\{ \rho_i^{-1} \left(\left[\sqrt{2 \beta_{2_i} \epsilon_{3_i}}, \infty \right] \right) \right\} \quad (54)$$

to ensure that the ultimate bound remains in the domain.

Theorem 1: For the dynamic model given in (1), the controller in (14), state estimator in (22), and FDI attack compensator in

(32) ensure semi-globally uniformly ultimately bounded tracking for each agent, in the sense that

$$\limsup_{t \rightarrow \infty} \|\Pi_i(t)\| \leq \sqrt{\frac{1}{\gamma_1} \left(H_{L_i, \max} + \frac{\gamma_2 \varphi_i}{\beta_2} \right)} \quad (55)$$

provided Assumptions 1–5 are satisfied and the sufficient conditions in (46) and (54) are satisfied.

Proof: Let $V_{L_i} : \mathcal{D}_i \rightarrow \mathbb{R}_{\geq 0}$ denote a positive definite, radially unbounded, and continuously differentiable Lyapunov candidate function defined as

$$\begin{aligned} V_{L_i} \triangleq & \frac{1}{2} e_i^T e_i + \frac{1}{2} r_i^T M_i r_i + \frac{1}{2} \tilde{q}_i^T \tilde{q}_i + \frac{1}{2} \tilde{r}_i^T \tilde{r}_i + P_{LK_i} \\ & + Q_{LK_i} + R_{LK_i} + H_{L_i}. \end{aligned} \quad (56)$$

The Lyapunov candidate function, V_{L_i} , can be bounded as

$$\gamma_1 \|\Pi_i\|^2 \leq V_{L_i} \leq \gamma_2 \|\Pi_i\|^2 + H_{L_i, \max}. \quad (57)$$

Taking the time derivative of (56) and substituting in \dot{e}_i , $\dot{\tilde{q}}_i$, $M_i \dot{r}_i$, and $\dot{\tilde{r}}_i$ from (7), (8), (17), and (25), applying the Leibniz Rule to (42)–(44), and using the fact that $\dot{\tilde{V}} = -\hat{V}$ and $\dot{\tilde{W}} = -\hat{W}$, yields

$$\begin{aligned} \dot{V}_{L_i} = & e_i^T (r_i - \beta_i e_i + A_i e_{u_i}) + r_i^T (-k_i M_i \eta_i r_i - k_i r_i - e_i \\ & + M_i \eta_i k_i r_{\tau_i} - k_i \dot{r}_i r_{\tau_i} - \frac{1}{2} \dot{M}_i r_i + \beta_i M_i A_i e_{u_i} \\ & - \dot{A}_i e_{u_i} + N_{1_i} + \chi_{1_i}) + \tilde{q}_i^T (\tilde{r}_i - \beta_i \tilde{q}_i) \\ & + \tilde{r}_i^T (-k_i \eta_i r_{\tau_i} - L_{2_i} \tilde{r}_i + L_{1_i} (S_i - \hat{S}_i) - \tilde{q}_i + \chi_{2_i} \\ & + N_{2_i}) + \left(\tau_i \omega_{1_i} \|u_i\|^2 - k_{1_i} \omega_{1_i} \int_{t-\tau_i}^t \|u_i(s)\|^2 ds \right) \\ & + (\omega_{2_i} \|r_i\|^2 - k_{1_i} \omega_{2_i} \|r_{\tau_i}\|^2) + (\tau_i \omega_{3_i} \|r_i\|^2 \\ & - k_{1_i} \omega_{3_i} \int_{t-\tau_i}^t \|r_i(s)\|^2 ds) + \frac{1}{2} r_i^T \dot{M}_i r_i \\ & - \text{tr}(\tilde{W}_i^T \Gamma_{1_i}^{-1} \dot{\tilde{W}}_i) - \text{tr}(\tilde{V}_i^T \Gamma_{2_i}^{-1} \dot{\tilde{V}}_i). \end{aligned} \quad (58)$$

The term $L_{1_i} \tilde{r}_i^T (S_i - \hat{S}_i)$ in (58) can be written as

$$\begin{aligned} L_{1_i} \tilde{r}_i^T (S_i - \hat{S}_i) &= L_{1_i} \Psi_{2_i}^T N_i - L_{1_i} N_i^T N_i \\ &= L_{1_i} \Psi_{2_i}^T \left(\tilde{W}_i^T \sigma(\hat{V}_i^T \delta_i) + \hat{W}_i^T \sigma'(\hat{V}_i^T \delta_i) \tilde{V}_i^T \delta_i \right) \\ &+ L_{1_i} (\tilde{r}_i + N_i)^T N_{n_i} - L_{1_i} N_i^T N_i. \end{aligned} \quad (59)$$

By utilizing (9), (11), (39), and (59), an upper bound on (58) can be obtained as

$$\begin{aligned} \dot{V}_{L_i} \leq & -\beta_i \|e_i\|^2 + a_i \|e_i\| \|e_{u_i}\| - k_i \|r_i\|^2 + k_i \bar{m}_i \bar{\eta}_i \|r_i\|^2 \\ & + k_i (\dot{\tau}_{Max} + \bar{m}_i \bar{\eta}_i k_{1_i}) \|r_i\| \|r_{\tau_i}\| + \|r_i\| \|\chi_{1_i}\| \\ & + \|r_i\| \|N_{1_i}\| - \beta_i \|\tilde{q}_i\|^2 - L_{2_i} \|\tilde{r}_i\|^2 + k_i \bar{\eta}_i \|\tilde{r}_i\| \|r_{\tau_i}\| \\ & + \|\tilde{r}_i\| \|\chi_{2_i}\| + \|\tilde{r}_i\| \|N_{2_i}\| + L_{1_i} \|\tilde{r}_i\| \|N_{n_i}\| \\ & + L_{1_i} \|N_i\| \|N_{n_i}\| + L_{1_i} \bar{m}_i^2 + \tau_i \omega_{1_i} k_i^2 \|r_i\|^2 \\ & + 2k_i^2 \tau_i \omega_{1_i} \|r_i\| \|N_i\| + \tau_i \omega_{1_i} k_i^2 \bar{m}_i^2 - k_{1_i} \omega_{2_i} \|r_{\tau_i}\|^2 \\ & - k_{1_i} \omega_{1_i} \int_{t-\tau_i}^t \|u_i(s)\|^2 ds + \omega_{2_i} \|r_i\|^2 + \tau_i \omega_{3_i} \|r_i\|^2 \\ & - k_{1_i} \omega_{3_i} \int_{t-\tau_i}^t \|r_i(s)\|^2 ds - \text{tr}(\tilde{W}_i^T \Gamma_{1_i}^{-1} \dot{\tilde{W}}_i) \\ & + (a_{d_i} + \beta_i \bar{m}_i a_i) \|r_i\| \|e_{u_i}\| - \text{tr}(\tilde{V}_i^T \Gamma_{2_i}^{-1} \dot{\tilde{V}}_i) \\ & + L_{1_i} \Psi_{2_i}^T \left(\tilde{W}_i^T \sigma(\hat{V}_i^T \delta_i) + \hat{W}_i^T \sigma'(\hat{V}_i^T \delta_i) \tilde{V}_i^T \delta_i \right). \end{aligned} \quad (60)$$

Substituting (37) and (38) into (60) cancels the term $L_{1_i} \Psi_{2_i}^T \left(\tilde{W}_i^T \sigma(\hat{V}_i^T \delta_i) + \hat{W}_i^T \sigma'(\hat{V}_i^T \delta_i) \tilde{V}_i^T \delta_i \right)$ in (60).

Young's inequality, the Cauchy–Schwarz inequality, and (40) can be utilized to upper bound select terms in (60). Furthermore, substituting gains (47)–(51) yields

$$\begin{aligned} \dot{V}_{L_i} \leq & -\alpha_{1_i} \|e_i\|^2 - \alpha_{2_i} \|r_i\|^2 - \beta_i \|\tilde{q}_i\|^2 - \alpha_{3_i} \|\tilde{r}_i\|^2 \\ & - \alpha_{4_i} \|e_{u_i}\|^2 - \alpha_{5_i} \|r_{\tau_i}\|^2 + \frac{1}{2\epsilon_{3_i}} \rho_i^2(\|z_i\|) \|z_i\|^2 \\ & - \frac{k_{1_i}}{2\tau_i} P_{LK_i} - \frac{k_{1_i} \omega_{3_i}}{2\omega_{2_i}} Q_{LK_i} - \frac{k_{1_i}}{2\tau_i} R_{LK_i} + \varphi_i, \end{aligned} \quad (61)$$

where $\rho_i^2(\|z_i\|) \triangleq \rho_{1_i}^2(\|z_i\|) + \rho_{2_i}^2(\|z_i\|)$ is a positive, globally invertible, nondecreasing function.

Considering Assumption 4, α_{5_i} can be designed to be positive. Therefore, the expression in (61) can be upper bounded as

$$\begin{aligned} \dot{V}_{L_i} \leq & -\left(\frac{\beta_{1_i}}{2} - \frac{1}{2\epsilon_{3_i}} \rho_i^2(\|z_i\|) \right) \|z_i\|^2 - \frac{\beta_{1_i}}{2} \|z_i\|^2 \\ & - \frac{k_{1_i}}{2\tau_i} P_{LK_i} - \frac{k_{1_i} \omega_{3_i}}{2\omega_{2_i}} Q_{LK_i} - \frac{k_{1_i}}{2\tau_i} R_{LK_i} + \varphi_i. \end{aligned} \quad (62)$$

The expression in (62) can be written as

$$\begin{aligned} \dot{V}_{L_i} \leq & -\left(\beta_{2_i} - \frac{1}{2\epsilon_{3_i}} \rho_i^2(\|z_i\|) \right) \|z_i\|^2 - \beta_{2_i} \|z_i\|^2 \\ & - \beta_{2_i} P_{LK_i} - \beta_{2_i} Q_{LK_i} - \beta_{2_i} R_{LK_i} + \varphi_i \\ \leq & -\left(\beta_{2_i} - \frac{1}{2\epsilon_{3_i}} \rho_i^2(\|z_i\|) \right) \|z_i\|^2 - \beta_{2_i} \|\Pi_i\|^2 + \varphi_i. \end{aligned} \quad (63)$$

Provided the initial condition in (53) is met and the sufficient condition in (54) is satisfied, then $\Pi_i \in \mathcal{D}_i$, and (57) can be used

to yield the following upper bound for (63):

$$\dot{V}_{L_i} \leq -\frac{\beta_{2_i}}{\gamma_{2_i}} V_{L_i} + \frac{\beta_{2_i}}{\gamma_{2_i}} H_{L_{i,\max}} + \varphi_i. \quad (64)$$

Using (57), the differential inequality in (64) can be solved to yield

$$\begin{aligned} V_{L_i}(t) &\leq V_{L_i}(t_0) \exp\left(-\frac{\beta_{2_i}}{\gamma_{2_i}}(t-t_0)\right) \\ &+ \left(H_{L_{i,\max}} + \frac{\gamma_{2_i}\varphi_i}{\beta_{2_i}}\right) \left(1 - \exp\left(-\frac{\beta_{2_i}}{\gamma_{2_i}}(t-t_0)\right)\right) \end{aligned} \quad (65)$$

$\forall t \in [t_0, \infty)$. Based on (57), the inequality in (65) can be written as

$$\begin{aligned} \|\Pi_i(t)\|^2 &\leq \frac{\gamma_{2_i}}{\gamma_{1_i}} \|\Pi_i(t_0)\|^2 \exp\left(-\frac{\beta_{2_i}}{\gamma_{2_i}}(t-t_0)\right) \\ &+ \frac{\gamma_{2_i}\varphi_i}{\gamma_{1_i}\beta_{2_i}} \left(1 - \exp\left(-\frac{\beta_{2_i}}{\gamma_{2_i}}(t-t_0)\right)\right) + \frac{1}{\gamma_{1_i}} H_{L_{i,\max}}. \end{aligned} \quad (66)$$

Using (66) yields the ultimate bound shown in (55), provided the sufficient conditions in (46) and (54) are satisfied, and provided that $\Pi_i(t_0) \in \mathcal{S}_{D_i}$. Given that $\Pi_i \in \mathcal{L}_\infty$, it can be proven that $e_i, r_i, \tilde{q}_i \in \mathcal{L}_\infty$, and (14) can be used to conclude that $u_i \in \mathcal{L}_\infty$.

VII. RESULTS

The control center of the centralized MAS is responsible for controlling each two-link manipulator. The performance of the proposed controller and detection algorithm for the nonlinear MAS under uncertainties, measurement noise, and FDI attacks is evaluated through a numerical simulation.⁴ For simplicity, during the simulation, each agent is given identical nonlinear dynamic models. The nonlinear dynamic model of the i th manipulator is described as

$$\begin{aligned} \begin{bmatrix} u_{1_i}(t - \tau_i) \\ u_{2_i}(t - \tau_i) \end{bmatrix} &= \begin{bmatrix} p_{1_i} + 2p_{3_i}c_{2_i} & p_{2_i} + p_{3_i}c_{2_i} \\ p_{2_i} + p_{3_i}c_{2_i} & p_{2_i} \end{bmatrix} \begin{bmatrix} \ddot{q}_{1_i} \\ \ddot{q}_{2_i} \end{bmatrix} \\ &+ \begin{bmatrix} -p_{3_i}s_{2_i}\dot{q}_{2_i} & -p_{3_i}s_{2_i}(\dot{q}_{1_i} + \dot{q}_{2_i}) \\ p_{3_i}s_{2_i}\dot{q}_{1_i} & 0 \end{bmatrix} \begin{bmatrix} \dot{q}_{1_i} \\ \dot{q}_{2_i} \end{bmatrix} \\ &+ \begin{bmatrix} f_{d1_i} & 0 \\ 0 & f_{d2_i} \end{bmatrix} \begin{bmatrix} \dot{q}_{1_i} \\ \dot{q}_{2_i} \end{bmatrix} + \begin{bmatrix} d_{1_i} \\ d_{2_i} \end{bmatrix}, \forall i \in [1, 2] \end{aligned} \quad (67)$$

where for $i \in \{1, 2, 3, 4\}$ $c_{2_i} \triangleq \cos(y_{2_i})$, $s_{2_i} \triangleq \sin(y_{2_i})$, $p_{1_i} = 3.473 \text{ kg m}^2$, $p_{2_i} = 0.196 \text{ kg m}^2$, $p_{3_i} = 0.242 \text{ kg m}^2$, $f_{d1_i} = 5.3 \text{ Nm s}$, $f_{d2_i} = 1.1 \text{ Nm s}$, $y_{j_i} \triangleq \pi_i(q_{j_i}, S_{1_i}) \forall j \in \{1, 2\}$,

⁴In practice, the design parameters can be selected based on experiments, simulations, prior history, or expert knowledge. The user-defined control gain k_i affects the tracking error, and it should be selected based on the actuator's practical limitation. The observer gains L_{1_i} and L_{2_i} affect the state estimation tracking error. The parameters Γ_{1_i} , Γ_{2_i} , and the number of neurons affect the FDI attack estimation accuracy. Only three neurons are used in the simulations, to achieve effective adaptation and detection. The tanh activation function is used in the NN implementation.

TABLE I
ROOT-MEAN-SQUARE ERROR (RMSE) OF THE POSITION TRACKING ERRORS IN THE PRESENCE OF AN FDI ATTACK

	Traditional controller	Proposed controller
Robot 1	0.028	0.008
Robot 2	0.041	0.013
Robot 3	0.026	0.009
Robot 4	0.015	0.01

and $\dot{y}_{j_i} \triangleq \pi_i(\dot{q}_{j_i}, S_{2_i}) \forall j \in \{1, 2\}$. Each of the agents has the following additive exogenous disturbance $d_{1_i} = 0.2\sin(0.1t)$ deg and $d_{2_i} = 0.1\sin(0.25t)$ deg.

The desired trajectories for each link of the first, third, and fourth robots are selected as $q_{d1_i} = 50\cos(1.5t)(1 - e^{-0.01t^3})$ deg, $q_{d2_i} = 30\cos(1.5t)(1 - e^{-0.01t^3})$ deg, and the desired trajectories for the links of the second robot are selected as $q_{d1_2} = [30\sin(1.5t) + 20](1 - e^{-0.01t^3})$ deg, $q_{d2_2} = [20\sin(0.5t) + 10](1 - e^{-0.01t^3})$ deg.

We assume that the control commands are transmitted to each robot with a time-varying time-delay of $\tau_i = 2\sin(t/2) + 3$ ms. The FDI attacks $S_{j_i}, \forall j \in \{1, 2\}, \forall i \in \{1, 2, 3, 4\}$, are injected to the j th link and the i th robot. The FDI attacks for the first robot are

$$S_{1_1} = \begin{cases} -0.5\sin(t) + \theta_{1_1}(t) \text{ deg}, & \text{if } t < 10 \\ 1 + \theta_{1_1}(t) \text{ deg}, & \text{if } 10 \leq t < 25 \\ -\sin(2t) + \theta_{1_1}(t) \text{ deg}, & \text{if } t \geq 25 \end{cases} \quad (68)$$

$$S_{2_1} = \begin{cases} -4\sin(t) + \theta_{2_1}(t), & \text{if } t < 10 \\ 7 + \theta_{2_1}(t) \text{ deg}, & \text{if } 10 \leq t < 30 \\ -7\sin(2t) + \theta_{2_1}(t) \text{ deg}, & \text{if } t \geq 30 \end{cases} \quad (69)$$

the FDI attacks applied to the second robot are

$$S_{1_2} = \begin{cases} 0 + \theta_{1_2}(t), & \text{if } t < 5 \\ -2 + \theta_{1_2}(t) \text{ deg}, & \text{if } 5 \leq t < 20 \\ -5\sin(2t) + \theta_{1_2}(t) \text{ deg}, & \text{if } t \geq 20 \end{cases} \quad (70)$$

$$S_{2_2} = \begin{cases} 0 + \theta_{2_2}(t), & \text{if } t < 5 \\ 1 + \theta_{2_2}(t) \text{ deg}, & \text{if } 5 \leq t < 20 \\ 1.5 + \theta_{2_2}(t) \text{ deg}, & \text{if } t \geq 20 \end{cases} \quad (71)$$

the FDI attacks applied to the third robot are

$$S_{1_3} = \begin{cases} 1 + \theta_{1_3}(t) \text{ deg}, & \text{if } t < 30 \\ 0 + \theta_{1_3}(t) \text{ deg}, & \text{if } t \geq 30 \end{cases} \quad (72)$$

$$S_{2_3} = \begin{cases} 7 + \theta_{2_3}(t) \text{ deg}, & \text{if } t < 30 \\ 0 + \theta_{2_3}(t) \text{ deg}, & \text{if } t \geq 30 \end{cases} \quad (73)$$

and the FDI attacks applied to the fourth robot are $S_{1_4} = \text{pulse}(1, 2, 5) + \theta_{1_4}$, where $S_{2_4} = 0 + \theta_{2_4}$ for $t > 0$, $\theta_{i_j}, j \in \{1, 2\}, \forall i \in \{1, 2, 3, 4\}$ denotes Gaussian noise, and the $\text{pulse}(a, b, c)$ represents a pulse generator function with amplitude of a , period of b seconds, and pulsewidth of c percent.

Table I illustrates the agent's tracking error in the presence of FDI attacks on the system's sensors and compares the performance of the developed and traditional control algorithms

TABLE II
RMSE FOR TIME-VARYING TIME-DELAY MAGNITUDES AND RATES OF FIRST ROBOT

Time Delay	$\tau_1(t)$ (ms)	RMSE
Small, Fast	$2\sin(\frac{t}{2}) + 3$	0.0084
Large, Fast	$20\sin(\frac{t}{2}) + 30$	0.0101
Small, Slow	$2\sin(\frac{t}{20}) + 3$	0.0085
Large, Slow	$20\sin(\frac{t}{20}) + 30$	0.0113

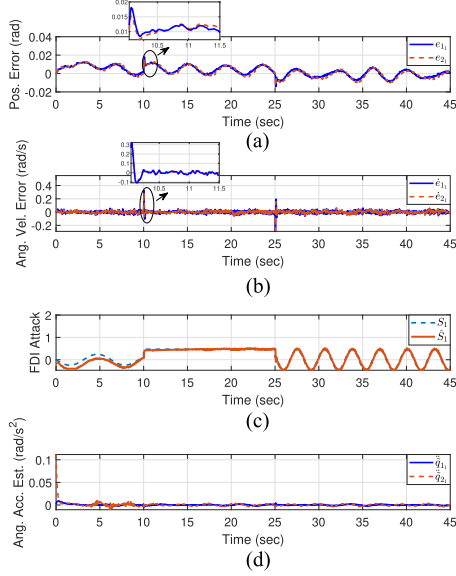


Fig. 3. (a) Position error, (b) angular velocity error, (c) FDI attack estimation, and (d) angular acceleration estimation error for Robot 1.

with each other. The traditional controller refers to a controller without FDI attack estimation [i.e., the term \hat{S}_i is set to zero in (12) and (23)]. The developed controller is able to track the desired position about $3 \times$ more accurately than the traditional controller. We further illustrate the robustness of the proposed approach by implementing a variety of time-varying input delays on the first robot and calculate the root-mean-square error (RMSE), as summarized in Table II. The results show that the system's performance is dependent on the delay amplitude, but not on the delay frequency. The tracking performance worsens as the magnitude of the input delay increases.

The position and angular velocity errors for both links of first and second robots are shown in Figs. 3 and 4, respectively. The estimation of the effect of the FDI attack is shown in Figs. 3(c) and 4(c), respectively, which illustrate the accuracy of the developed attack estimation algorithm. Figs. 3(d) and 4(d) illustrate the angular acceleration estimation errors. The position tracking error of the first robot remains between -0.02 and 0.02 rad under FDI attacks, measurement noise, input delays, and additive disturbances. The angular velocity error of the first robot remains between -0.01 and 0.01 rad/s. The estimator was able to estimate the injected FDI attack accurately. The observer is able to estimate the state variables accurately, as shown in Figs. 3(d) and 4(d). The FDI attack estimator is able to estimate negative faults as shown in Fig. 4(c). The proposed

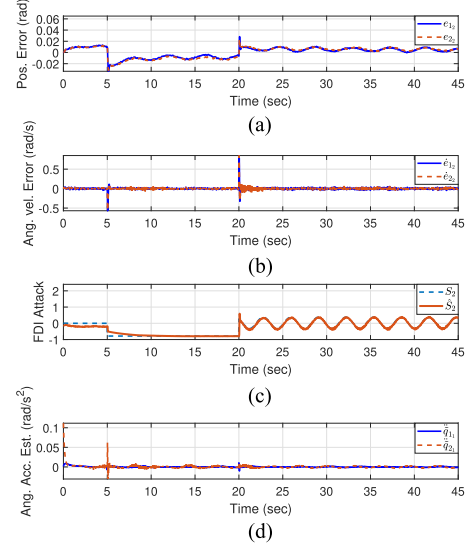


Fig. 4. (a) Position error, (b) angular velocity error, (c) FDI attack estimation, and (d) angular acceleration estimation error for Robot 2.

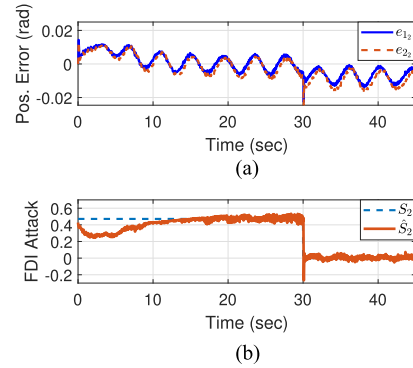


Fig. 5. Position error and FDI attack estimation for Robot 3.

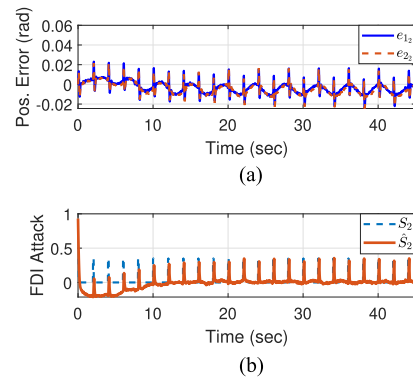


Fig. 6. Position error and FDI attack estimation for Robot 4.

FDI attack estimation approach can estimate constant, periodic, and pulse train of FDI attacks accurately. The position error and FDI attack estimation for the third and fourth robots are shown in Figs. 5 and 6, respectively. The controller was able to track the desired signals for the third robot accurately, as shown in

Fig. 5(a). A spike occurs at 30 s due to the sudden changes in the injected FDI attack. The magnitude of the spike can be reduced by modifying the FDI attack estimator gains. However, the FDI attack estimation performance decreases with decreasing the NN gains. Fig. 6(b) shows that the proposed FDI attack estimator can detect an FDI attack that is injected as a pulse-train. The tracking error remains between 0.02 and -0.02 rad as shown in Fig. 6(a). The developed controller is able to compensate for the effect of FDI attacks in real time. There are spikes in position and angular velocity errors at time 10 and 25 s for the first robot, at time 5 and 20 s for the second robot, and at time 30 s for the third robot, which occur due to the fact that the attacks are injected abruptly to the links. However, the controller is able to compensate for the attack in a short amount of time. The results suggest that the proposed controller is robust to input delay, FDI attacks, and additive disturbances.

A. Discussion

Learning-based methods alone cannot accurately estimate FDI attacks in real time for nonlinear systems under measurement noise and input delays, whereas model-based methods require accurate knowledge of the system. Combining the learning and model-based methods lowered the RMSE significantly, indicating that the developed method is robust to uncertainties; hence, the anomaly detection algorithm is able to estimate the effect of FDI attacks accurately and promptly. As shown in the simulation results, the developed FDI attack estimation algorithm can detect and estimate simultaneous attacks on different system links. Since the developed control strategy uses the nonlinear model of the system, it can compensate for attacks that are injected at the initial simulation time.

VIII. CONCLUSION

A centralized anomaly detection, state estimation, and control strategy was developed to be robust to a time-varying input delay, measurement noise, and FDI attacks. The developed attack detection algorithm consisted of a nonlinear model-based observer and an NN observer to mitigate the adverse effects of FDI attacks in real time. The update laws for the NN weights are designed based on a Lyapunov stability analysis. The performance of the developed controller was evaluated through simulation for a MAS composed of four two-link planar manipulators. The FDI attack estimator was able to accurately estimate the FDI attack in real time. The proposed detection and mitigation strategy can detect and estimate FDI attacks applied at the initial simulation time despite learning-based techniques.

IX. FUTURE WORK

The dependency of the proposed approach to the parameter β_i is one of the limitations of the proposed technique, which will be investigated in future works. Future works may also investigate the development of a control design for agents with unknown dynamics. Adaptive control techniques and event-based control can also be considered in future work. Additionally, partially observable systems can also be investigated. Improvements to

the proposed work can also be made by developing controllers that utilize intermittent communication. Furthermore, future work may focus on extending the proposed control design for distributed MASs.

REFERENCES

- [1] H. Shayeghi, H. Shayanfar, and A. Jalili, "Load frequency control strategies: A state-of-the-art survey for the researcher," *Energy Convers. Manage.*, vol. 50, no. 2, pp. 344–353, 2009.
- [2] A. Sargolzaei, A. Abbaspour, M. A. Al Faruque, A. S. Eddin, and K. Yen, "Security challenges of networked control systems," in *Sustainable Interdependent Networks*. Springer, 2018, pp. 77–95. [Online]. Available: https://doi.org/10.1007/978-3-319-74412-4_6
- [3] O. Kosut, L. Jia, R. J. Thomas, and L. Tong, "Malicious data attacks on the smart grid," *IEEE Trans. Smart Grid*, vol. 2, no. 4, pp. 645–658, Dec. 2011.
- [4] Y. Liu, P. Ning, and M. K. Reiter, "False data injection attacks against state estimation in electric power grids," *ACM Trans. Inf. Syst. Secur.*, vol. 14, no. 1, pp. 1–33, 2011.
- [5] M. Al Janaideh, E. Hammad, A. Farraj, and D. Kundur, "Mitigating attacks with nonlinear dynamics on actuators in cyber-physical mechatronic systems," *IEEE Trans. Ind. Informat.*, vol. 15, no. 9, pp. 4845–4856, Sep. 2019.
- [6] W. Ao, Y. Song, and C. Wen, "Adaptive cyber-physical system attack detection and reconstruction with application to power systems," *IET Control Theory Appl.*, vol. 10, no. 12, pp. 1458–1468, 2016.
- [7] H. M. Khalid and J. C.-H. Peng, "Immunity toward data-injection attacks using multisensor track fusion-based model prediction," *IEEE Trans. Smart Grid*, vol. 8, no. 2, pp. 697–707, Mar. 2017.
- [8] R. Deng, G. Xiao, and R. Lu, "Defending against false data injection attacks on power system state estimation," *IEEE Trans. Ind. Informat.*, vol. 13, no. 1, pp. 198–207, Feb. 2017.
- [9] Z.-H. Yu and W.-L. Chin, "Blind false data injection attack using PCA approximation method in smart grid," *IEEE Trans. Smart Grid*, vol. 6, no. 3, pp. 1219–1226, May 2015.
- [10] K. Manandhar, X. Cao, F. Hu, and Y. Liu, "Detection of faults and attacks including false data injection attack in smart grid using Kalman filter," *IEEE Trans. Control Netw. Syst.*, vol. 1, no. 4, pp. 370–379, Dec. 2014.
- [11] Z.-H. Pang, G.-P. Liu, D. Zhou, F. Hou, and D. Sun, "Two-channel false data injection attacks against output tracking control of networked systems," *IEEE Trans. Ind. Electron.*, vol. 63, no. 5, pp. 3242–3251, May 2016.
- [12] P. Bangalore and L. B. Tjernberg, "An artificial neural network approach for early fault detection of gearbox bearings," *IEEE Trans. Smart Grid*, vol. 6, no. 2, pp. 980–987, Mar. 2015.
- [13] A. Abdullah, "Ultrafast transmission line fault detection using a DWT based ANN," *IEEE Trans. Ind. Appl.*, vol. 54, no. 2, pp. 1182–1193, Mar./Apr. 2018.
- [14] S. Jana and A. De, "A novel zone division approach for power system fault detection using ANN-based pattern recognition technique," *Canadian J. Elect. Comput. Eng.*, vol. 40, no. 4, pp. 275–283, 2017.
- [15] M. Ozay, I. Esnaola, F. T. Y. Vural, S. R. Kulkarni, and H. V. Poor, "Machine learning methods for attack detection in the smart grid," *IEEE Trans. Neural Netw. Learn. Syst.*, vol. 27, no. 8, pp. 1773–1786, Aug. 2016.
- [16] J. Yan, H. He, X. Zhong, and Y. Tang, "Q-learning-based vulnerability analysis of smart grid against sequential topology attacks," *IEEE Trans. Inf. Forensics Secur.*, vol. 12, no. 1, pp. 200–210, Jan. 2017.
- [17] S. A. Foroutan and F. R. Salmasi, "Detection of false data injection attacks against state estimation in smart grids based on a mixture gaussian distribution learning method," *IET Cyber-Phys. Syst.: Theory Appl.*, vol. 2, no. 4, pp. 161–171, 2017.
- [18] Y. He, G. J. Mendis, and J. Wei, "Real-time detection of false data injection attacks in smart grid: A deep learning-based intelligent mechanism," *IEEE Trans. Smart Grid*, vol. 8, no. 5, pp. 2505–2516, Sep. 2017.
- [19] J. Hao, R. J. Piechocki, D. Kaleshi, W. H. Chin, and Z. Fan, "Sparse malicious false data injection attacks and defense mechanisms in smart grids," *IEEE Trans. Ind. Informat.*, vol. 11, no. 5, pp. 1–12, Oct. 2015.
- [20] Z. Kazemi, A. A. Safavi, F. Naseri, L. Urbas, and P. Setoodeh, "A secure hybrid dynamic-state estimation approach for power systems under false data injection attacks," *IEEE Trans. Ind. Informat.*, vol. 16, no. 12, pp. 7275–7286, Dec. 2020.
- [21] M. Khalaf, A. Youssef, and E. El-Saadany, "Joint detection and mitigation of false data injection attacks in AGC systems," *IEEE Trans. Smart Grid*, vol. 10, no. 5, pp. 4985–4995, Sep. 2019.

- [22] A. Sargolzaei, K. Yazdani, A. Abbaspour, C. D. Crane III, and W. E. Dixon, "Detection and mitigation of false data injection attacks in networked control systems," *IEEE Trans. Ind. Informat.*, vol. 16, no. 6, pp. 4281–4292, Jun. 2020.
- [23] A. Abbaspour, P. Aboutalebi, K. K. Yen, and A. Sargolzaei, "Neural adaptive observer-based sensor and actuator fault detection in nonlinear systems: Application in UAV," *ISA Trans.*, vol. 67, pp. 317–329, 2017, doi: [10.1016/j.isatra.2016.11.005](https://doi.org/10.1016/j.isatra.2016.11.005).
- [24] X.-X. Ren and G.-H. Yang, "Adaptive control for nonlinear cyber-physical systems under false data injection attacks through sensor networks," *Int. J. Robust Nonlinear Control*, vol. 30, no. 1, pp. 65–79, 2020.
- [25] W. He, F. Qian, Q.-L. Han, and G. Chen, "Almost sure stability of nonlinear systems under random and impulsive sequential attacks," *IEEE Trans. Autom. Control*, vol. 65, no. 9, pp. 3879–3886, Sep. 2020.
- [26] J. Kim, C. Lee, H. Shim, Y. Eun, and J. H. Seo, "Detection of sensor attack and resilient state estimation for uniformly observable nonlinear systems having redundant sensors," *IEEE Trans. Autom. Control*, vol. 64, no. 3, pp. 1162–1169, Mar. 2019.
- [27] W. He, X. Gao, W. Zhong, and F. Qian, "Secure impulsive synchronization control of multi-agent systems under deception attacks," *Inf. Sci.*, vol. 459, pp. 354–368, 2018, doi: [10.1016/j.ins.2018.04.020](https://doi.org/10.1016/j.ins.2018.04.020).
- [28] N. Sharma, S. Bhasin, Q. Wang, and W. E. Dixon, "Predictor-based control for an uncertain Euler–Lagrange system with input delay," *Automatica*, vol. 47, no. 11, pp. 2332–2342, 2011.
- [29] N. Fischer, A. Dani, N. Sharma, and W. E. Dixon, "Saturated control of an uncertain nonlinear system with input delay," *Automatica*, vol. 49, no. 6, pp. 1741–1747, 2013.
- [30] S. Obuz, J. R. Klotz, R. Kamalapurkar, and W. E. Dixon, "Unknown time-varying input delay compensation for uncertain nonlinear systems," *Automatica*, vol. 76, pp. 222–229, Feb. 2017, doi: [10.1016/j.automatica.2016.09.030](https://doi.org/10.1016/j.automatica.2016.09.030).
- [31] D. Sorensen, "Design and control of a space based two link manipulator with Lyapunov based control laws," Naval Postgraduate School, Tech. Rep., 1992. [Online]. Available: <https://calhoun.nps.edu/handle/10945/23618>
- [32] H. Fukusho, T. Koseki, and T. Sugimoto, "Control of a straight line motion for a two-link robot arm using coordinate transform of bi-articular simultaneous drive," in *Proc. IEEE 11th Int. Workshop Adv. Motion Control*, 2010, pp. 786–791.
- [33] J. Wang, F. Wang, G. Wang, S. Li, and L. Yu, "Generalized proportional integral observer based robust finite control set predictive current control for induction motor systems with time-varying disturbances," *IEEE Trans. Ind. Informat.*, vol. 14, no. 9, pp. 4159–4168, Sep. 2018.
- [34] S. Oh and K. Kong, "Two-degree-of-freedom control of a two-link manipulator in the rotating coordinate system," *IEEE Trans. Ind. Electron.*, vol. 62, no. 9, pp. 5598–5607, Sep. 2015.
- [35] S. Zhang, X. Zhao, Z. Liu, and Q. Li, "Boundary torque control of a flexible two-link manipulator and its experimental investigation," *IEEE Trans. Ind. Electron.*, vol. 68, no. 9, pp. 8708–8717, Sep. 2021.
- [36] J. Richardson, J. Korniak, P. D. Reiner, and B. M. Wilamowski, "Nearest-neighbor spline approximation (NNSA) improvement to TSK fuzzy systems," *IEEE Trans. Ind. Informat.*, vol. 12, no. 1, pp. 169–178, Feb. 2016.
- [37] A. Malinowski and H. Yu, "Comparison of embedded system design for industrial applications," *IEEE Trans. Ind. Informat.*, vol. 7, no. 2, pp. 244–254, May 2011.
- [38] W. He and Y. Dong, "Adaptive fuzzy neural network control for a constrained robot using impedance learning," *IEEE Trans. Neural Netw. Learn. Syst.*, vol. 29, no. 4, pp. 1174–1186, Apr. 2018.
- [39] L. Liu, Y.-J. Liu, A. Chen, S. Tong, and C. P. Chen, "Integral barrier Lyapunov function-based adaptive control for switched nonlinear systems," *Sci. China Inf. Sci.*, vol. 63, no. 3, pp. 1–14, 2020.
- [40] D.-J. Li, J. Li, and S. Li, "Adaptive control of nonlinear systems with full state constraints using integral barrier Lyapunov functionals," *Neurocomputing*, vol. 186, pp. 90–96, 2016, doi: [10.1016/j.neucom.2015.12.075](https://doi.org/10.1016/j.neucom.2015.12.075).
- [41] N. Fischer, R. Kamalapurkar, N. Fitz-Coy, and W. E. Dixon, "Lyapunov-based control of an uncertain Euler–Lagrange system with time-varying input delay," in *Proc. Amer. Control Conf.*, 2012, pp. 3919–3924.
- [42] W. E. Dixon, A. Behal, D. M. Dawson, and S. P. Nagarkatti, *Nonlinear Control of Engineering Systems: A Lyapunov-Based Approach*. Berlin, Germany: Springer Science & Business Media, 2013.
- [43] N. Bekiaris-Liberis and M. Krstic, "Compensation of time-varying input and state delays for nonlinear systems," *J. Dyn. Syst., Meas., Control*, vol. 134, no. 1, 2012, Art. no. 011009.
- [44] D. Bresch-Pietri and M. Krstic, "Delay-adaptive control for nonlinear systems," *IEEE Trans. Autom. Control*, vol. 59, no. 5, pp. 1203–1218, May 2014.
- [45] N. E. Cotter, "The Stone–Weierstrass theorem and its application to neural networks," *IEEE Trans. Neural Netw.*, vol. 1, no. 4, pp. 290–295, Dec. 1990.
- [46] R. R. Selmic and F. L. Lewis, "Neural-network approximation of piecewise continuous functions: Application to friction compensation," *IEEE Trans. Neural Netw.*, vol. 13, no. 3, pp. 745–751, May 2002.
- [47] M. Krstic, P. V. Kokotovic, and I. Kanellakopoulos, *Nonlinear and Adaptive Control Design*. Hoboken, NJ, USA: Wiley, 1995.